

# Detection of $\gamma$ -Aminobutyric Acid (GABA) by Longitudinal Scalar Order Difference Editing

Robin A. de Graaf and Douglas L. Rothman

*Magnetic Resonance Center, Department of Diagnostic Radiology, Yale University School of Medicine, New Haven, Connecticut 06520-8043*

E-mail: [robin.degraaf@yale.edu](mailto:robin.degraaf@yale.edu)

Received January 26, 2001; revised May 7, 2001; published online July 6, 2001

**Two novel spectral editing techniques for the *in vivo* detection of  $\gamma$ -aminobutyric acid (GABA) are presented. The techniques rely on the generation of longitudinal scalar order (LSO) coherences, which in combination with *J*-difference editing results in the selective detection of GABA. The utilization of LSO coherences makes the editing sequences insensitive to phase and frequency instabilities. Furthermore, the spectral editing selectivity can be increased independent of the echo time, thereby opening the echo time for state-of-the-art water suppression and/or spatial localization techniques. The performance of the LSO editing techniques is theoretically demonstrated with product operator calculations and density matrix simulations and experimentally evaluated on phantoms *in vitro* and on human brain *in vivo*.** © 2001 Academic Press

**Key Words:**  $\gamma$ -aminobutyric acid (GABA); longitudinal scalar order; spectral editing; <sup>1</sup>H NMR spectroscopy; human brain.

## INTRODUCTION

$\gamma$ -aminobutyric acid (GABA) is the major inhibitory neurotransmitter in the mammalian brain (1). GABA is essential for normal brain function. Dysfunction of GABAergic neurotransmission has implications in many neurological and physiological diseases, such as epilepsy, depression, and schizophrenia (2–4). The ability to monitor GABA concentrations *in vivo* would represent a substantial advance in the monitoring of these diseases and of various drug therapies. <sup>1</sup>H NMR spectroscopy (MRS) offers a technique for noninvasively measuring GABA concentrations in human cerebral cortex and animal brain *in vivo* (5, 6). However, the narrow chemical shift dispersion of  $\sim 3$  ppm (for the majority of metabolite resonances) leads to severe spectral overlap of resonances. Specifically, the three resonances of GABA are overlapping with *N*-acetyl aspartate, glutamate, glutamine, or total creatine (=sum of creatine and phosphorylated creatine), making direct GABA detection by <sup>1</sup>H MRS impossible. The problem of spectral overlap is commonly solved by employing spectral editing techniques that utilize a difference in scalar coupling to selectively observe the resonance(s) of interest. Previous *in vivo* GABA spectral editing techniques were, among others, based on *J*-difference editing (5–8) or multiple

quantum-coherences (9, 10). Although theoretically all techniques should achieve adequate spectral editing, many of the previously established techniques suffer from incomplete water suppression and spatial localization or insufficient spectral selectivity.

Here we present a spectral editing technique for *in vivo* detection of GABA based on the combination of longitudinal scalar order editing (11, 12) and *J*-difference editing (5–8). The technique achieves spectral editing along the longitudinal axis, thereby eliminating any phase-related artifacts and opening the echo-time period for state-of-the-art water suppression and/or localization. Furthermore, the sequence can be (partially) executed with adiabatic RF pulses for minimal sensitivity to RF inhomogeneities. Although the technique is presented for GABA, it performs equally well for other (weakly coupled) spin systems such as lactate, alanine, and beta-hydroxy butyrate.

## THEORY

GABA (H<sub>2</sub>NCH<sub>2</sub>CH<sub>2</sub>CH<sub>2</sub>COOH) may be approximated as an  $A_2M_2X_2$  spin system with GABA-H4 ( $A_2$ ) resonating as a triplet at 3.01 ppm, GABA-H3 ( $M_2$ ) as a quintet at 1.89 ppm, and GABA-H2 ( $X_2$ ) as a triplet at 2.28 ppm (with a *J* coupling constant of  $\sim 7.3$  Hz for all interactions). This description is accompanied by two assumptions. Firstly, the amide and carbonyl protons are in rapid exchange with water and are hence NMR invisible. Secondly, it is assumed that GABA can be described as a weakly coupled spin system. Although this assumption is not valid for the interaction between the GABA-H2 and GABA-H3 protons at 2.1 T (89.64 MHz), it is a reasonable approximation for the GABA-H3/H4 interaction. Therefore, in further calculations the weak-coupling approximation will be maintained, after which any deviation from ideal behavior due to strong coupling effects will be discussed.

The basic versions of the proposed sequences are shown in Figs. 1A and 1B. First consider the sequence in Fig. 1A. Following nonselective excitation, the transverse magnetization evolves under the effects of *J* coupling, frequency offsets,  $B_0$

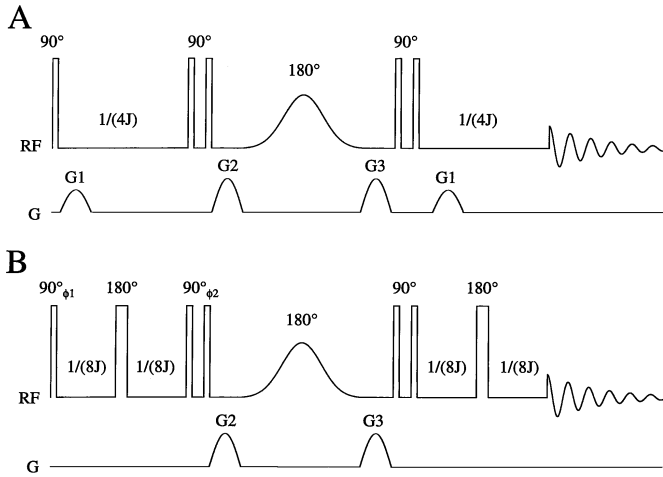


**FIG. 1.** Basic NMR pulse sequences for (A) incoherent and (B) coherent longitudinal scalar order (LSO) editing. The second and third  $90^\circ$  pulses in both sequences are executed as semi-selective jump–return pulses, with a null on the  $M$  spins (GABA-H3) and maximum excitation at the  $A$  spins (GABA-H4). The  $180^\circ$  inversion pulse is selective for the  $M$  spins. The magnetic field gradient G2 ensures that only longitudinal magnetization passes the editing element by dephasing all transverse magnetization. The magnetic field gradient G3 dephases all magnetization excited by the (imperfect)  $180^\circ$  inversion pulse. In order to avoid unwanted signal refocusing,  $G2 \neq G3$ . For GABA (or  $AX_2$  spin systems), the total echo time TE equals  $1/(2J)$ . For  $AX$  and  $AX_3$  spin systems,  $TE = 1/J$ . Theoretically,  $\phi_1 = \phi_2$  during cLSO editing for optimal GABA detection. However, in practice the phases must be calibrated for optimal editing performance.

magnetic field inhomogeneities, and magnetic field gradients. The second pulse is a semi-selective jump–return pulse (centered on the  $M$  spins), which rotates the magnetization over a frequency-dependent nutation angle  $\alpha$ , where  $\alpha(\nu) = (\pi/2)[(\nu - \nu_M)/|\nu_A - \nu_M|]$ .  $\nu_A$  and  $\nu_M$  are the frequencies of the  $A$  and  $M$  spins, respectively. Therefore, the  $M$  spins are left unperturbed ( $\alpha = 0^\circ$  for  $\nu = \nu_M$ ), while off-resonance spins are rotated over an angle  $\alpha$ . The subsequent magnetic field gradient dephases all transverse coherences, leaving the coherences of interest along the longitudinal axis. Note that, since the transverse magnetization is dephased prior to the second  $90^\circ$  pulse, at most 50% (for  $\alpha = 90^\circ$ ) of the coherences can be rotated to the longitudinal axis. The 50% signal loss is inherent to all stimulated echo-acquisition sequences (13). The  $180^\circ$  pulse selectively inverts the  $M$  (GABA-H3) protons in subsequent experiments. Note that only longitudinal coherences associated with an odd number of  $M$  spins (e.g.,  $A_y(M_{z,1} + M_{z,2})$ ) are sensitive (i.e., invert) to the selective  $180^\circ$  pulse. Following selective excitation of the longitudinal scalar order coherences, the transverse coherences are rephased during the second evolution delay  $t$ . In the absence of selective inversion of the GABA-H3 spins, the density matrix at the top of the echo (14) is given by

$$\sigma(\text{TE}) = \frac{1}{2} A_x \sin^2 \alpha. \quad [1]$$

In the presence of selective inversion of the GABA-H3 protons, the coherences at the top of the echo are given by

$$\begin{aligned} \sigma(\text{TE}) = & \frac{1}{2} [A_x \cos^2 \pi J \text{TE} + 2A_y(M_{z,1} + M_{z,2}) \\ & \times \sin \pi J \text{TE} \cos \pi J \text{TE} \\ & - 4A_x M_{z,1} M_{z,2} \sin^2 \pi J \text{TE}] \sin^2 \alpha, \quad [2] \end{aligned}$$

which reduces to  $-2A_x M_{z,1} M_{z,2} \sin^2 \alpha$  for  $\text{TE} = 1/(2J) = 68$  ms. The experiment can be optimized for GABA-H4 editing by making  $\alpha$  equal to  $90^\circ$ . Therefore, in the second experiment an anti-phase triplet resonance ( $-2A_x M_{z,1} M_{z,2}$ ) for GABA-H4 in which the outer resonances are negative is obtained. Subtracting this from the in-phase triplet ( $A_x$ ) resonance obtained in the first experiment gives the outer resonances of the GABA-H4 triplet. Therefore, this sequence recovers 25% of the total integrated signal of GABA; 50% cannot be recovered due to the stimulated echo nature of the sequence and another 50% is lost since the inner resonance of GABA does not modulate as a function of the echo time. The loss of 50% due to the absence of modulation of the inner resonance is also inherent in spin-echo  $J$  editing sequences (5–8). For  $AX$  and  $AX_3$  spin systems, the complete multiplet structure can be inverted at  $\text{TE} = 1/J$ , such that 50% of the total integrated signal can be recovered. Since the coherences are incoherent during the editing element, the sequence will be referred to as incoherent longitudinal scalar order (iLSO) spectral editing.

Figure 1B shows the basic sequence for coherent longitudinal scalar order (cLSO) spectral editing. The sequence is similar to the iLSO sequence, with the essential difference of two refocusing pulses during the evolution periods and a strict phase relation between the first and second  $90^\circ$  pulses. Following excitation and the evolution period  $t$  the coherences are not effected by static or applied magnetic field gradients and have only evolved due to  $J$  coupling effects. To create the desired longitudinal scalar order coherences, the semi-selective  $90^\circ$  pulse must be applied with a relative phase identical to the first excitation pulse. Coherences that are not brought to the longitudinal axis will be dephased by the subsequent magnetic field gradient. At this point it is important to realize that uncoupled spins are  $90^\circ$  out-of-phase with coherences of the coupled spin-of-interest. Therefore, uncoupled spins are not brought to the longitudinal axis and are dephased by the magnetic field gradient, thereby giving unwanted signal suppression in a single acquisition. Although the uncoupled resonances are theoretically suppressed in a single acquisition, an imperfect phase relation between the first two pulses (for example, due to residual magnetic field gradients) will cause some residual signal from uncoupled spins. However, this residual will be subtracted in the final difference spectrum. Following excitation and refocusing, the coherences at the top of the echo

are given by

$$\sigma(\text{TE}) = -[A_x \sin \pi J \text{TE} + 2A_y(M_{z,1} + M_{z,2}) \cos \pi J \text{TE} + 4A_x M_{z,1} M_{z,2} \sin \pi J \text{TE}] \sin^2 \alpha. \quad [3]$$

For  $\text{TE} = 1/(2J)$  and  $\alpha = 90^\circ$ , Eq. [3] reduces to  $-A_x - 4A_x M_{z,1} M_{z,2}$ , which represents the outer two resonance of GABA-H4. The inner GABA-H4 resonance essentially behaves as an uncoupled spin system and is suppressed in a single acquisition, as expected. When the GABA-H3 spins are selectively inverted, the coherences are given by

$$\sigma(\text{TE}) = [A_x \sin \pi J \text{TE} + 2A_y(M_{z,1} + M_{z,2}) \cos \pi J \text{TE} + 4A_x M_{z,1} M_{z,2} \sin \pi J \text{TE}] \sin^2 \alpha, \quad [4]$$

which reduces to  $+A_x + 4A_x M_{z,1} M_{z,2}$  for  $\text{TE} = 1/(2J)$  and  $\alpha = 90^\circ$ . Subtracting both experiments gives the outer resonances of GABA-H4. The cLSO sequence therefore achieves 50% editing efficiency of GABA, or  $AX_2$  spin systems in general, since the inner GABA-H4 resonance is suppressed. The cLSO editing efficiency for  $AX$  and  $AX_3$  spin systems is 100%.

## METHODS

Five healthy human subjects (four males, one female) were studied in accordance with Institutional Review Board guidelines for research in human subjects. All human experiments were performed on a 2.1-T magnet interfaced to a Bruker Avance spectrometer (Bruker Instruments Inc., Billerica, MA). The system was equipped with actively shielded gradients capable of switching 14.4 mT/m in 1.1 ms. Human subjects were placed supine on the magnet bed and the head was immobilized with foam in a specially designed head holder. RF transmission and signal reception were performed with an 8-cm-diameter single-turn surface coil. The exact spatial positions of the brain and the localized volume used for spectroscopy were determined from axial and sagittal multislice FLASH images. The homogeneity of the main magnetic field was optimized over a cubic volume covering the volume-of-interest by a modification of the FASTMAP routine (15, 16), generally resulting in water linewidths of 5–6 Hz.

The basic sequences shown in Fig. 1 must be extended with elements for water suppression and spatial localization. Figure 2 shows the LSO pulse sequences as implemented for *in vivo*  $^1\text{H}$  MRS. Spatial localization is achieved with the image-selected *in vivo* spectroscopy (ISIS) technique (17) in combination with outer volume suppression (OVS, 13). The ISIS inversion and OVS excitation pulses were 4-ms hyperbolic secant inversion pulses (bandwidth = 2.5 kHz). For iLSO editing, additional localization is achieved by replacing the initial nonselective excitation with a 1-ms slice-selective  $90^\circ$  SLR excitation pulse (13). Additional localization during the cLSO sequence was achieved

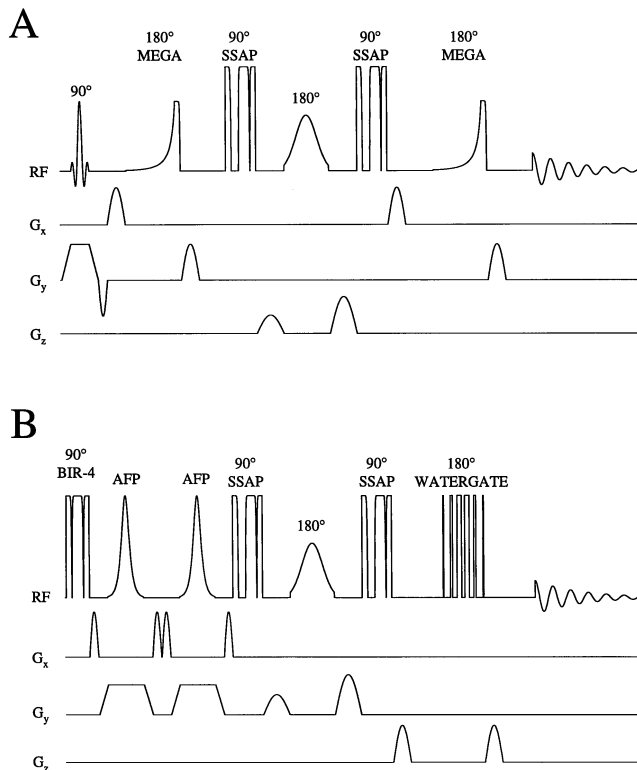


**FIG. 2.** Experimentally implemented (A) iLSO and (B) cLSO editing sequences. Both sequences are preceded by 3D ISIS and OVS localization, as well as three CHES elements for water suppression. Trapezoidal and sinusoidal magnetic field gradients are used for slice selection and coherence spoiling, respectively. Only the minimum required magnetic field gradients are shown. See the legend of Fig. 1 and the text for more details.

by a pair of two 4-ms slice-selective adiabatic full passage (AFP) pulses (bandwidth = 2.5 kHz). Extracranial lipid resonances were effectively removed with magnetic field gradient pulses from a planar surface gradient coil (18) following the last  $90^\circ$  pulse. The localized volume of  $3 \times 2 \times 3 \text{ cm}^3$  ( $x \times y \times z = 18 \text{ ml}$ ) was positioned in the occipital/parietal cortex, avoiding large blood vessels. Water suppression is achieved with three CHES elements (19) preceding the sequence. Each CHES element consisted of a 20-ms Gaussian RF pulse truncated at 10% followed by a 5-ms magnetic field gradient. Additional water suppression is achieved with the MEGA technique (20) for iLSO editing and the WATERGATE sequence (21) for cLSO editing. Specifically, the selective spin-echo dephasing technique MEGA was executed with 20-ms asymmetrical adiabatic full passage pulses (HS1/2,  $R = 10$ , 0.9 T;  $\tanh/\tan$ ,  $R = 100$ , 0.1 T, for nomenclature see (22)) as previously described for liquid-state high-resolution NMR (22). This asymmetric MEGA sequence provided excellent water suppression over a bandwidth of  $>100 \text{ Hz}$  with complete insensitivity to RF inhomogeneities as associated with surface coils (13). The asymmetric character of the MEGA pulses resulted in a high spectral selectivity with a  $\sim 70\text{-Hz}$  transition bandwidth between frequencies of

complete and negligible signal suppression. The WATERGATE sequence ( $3\alpha_{+x}-t-9\alpha_{+x}-t-19\alpha_{+x}-t-19\alpha_{-x}-t-9\alpha_{-x}-t-3\alpha_{-x}$ ,  $\alpha = 6.93^\circ$ ) was executed with a  $100 \mu\text{s}$  for a  $90^\circ$  pulse and the refocusing maximum at 200 Hz off-resonance ( $t = 2.5 \text{ ms}$ ). Due to the relatively long pulses, the intrapulse delays were corrected for chemical shift evolution during the pulses according to  $t_{\text{corrected}} = t - (2/\pi) \cdot T_{\text{total}}$ , where  $T_{\text{total}}$  is the combined length of the pulses immediately prior to and following that particular delay  $t$  (13).

All experiments were performed with a repetition time  $\text{TR} = 3000 \text{ ms}$ , an echo time  $\text{TE} = 68 \text{ ms}$  ( $=1/(2J_{\text{GABA H3-H4}})$ ) and  $\text{TM} = 35 \text{ ms}$  ( $\text{TM}$  equals the period in between the last two  $90^\circ$  pulses, when the magnetization is along the longitudinal axis, see Fig. 2). To balance the spectral selectivity with the generation and subsequent loss of coherences during the selective inversion pulse, a 20-ms Gaussian, truncated at 10%, was used (inversion bandwidth  $\sim 56 \text{ Hz}$ ). The selective inversion pulse was positioned on the GABA-H3 at 1.89 ppm and on a mirror position (4.13 ppm) relative to GABA-H4 at 3.01 ppm on alternate acquisitions. The alternate acquisitions were stored separately, for post-acquisition  $J$ -difference editing. The acquired FIDs were zero-filled to 8K data points, apodized (4 Hz Gaussian line broadening), Fourier transformed, and phase corrected (only zero order phase). The spectra were frequency shifted (maximum  $\pm 1 \text{ Hz}$ ) to account for drift in the main magnetic field, but no amplitude or phase corrections were allowed on individual spectra. The sensitivity of the sequences toward RF inhomogeneities was significantly decreased by replacing the classical jump–return  $90^\circ$  pulses by their adiabatic analogues (known as solvent suppression adiabatic pulses, or SSAP (23)). The 2-ms SSAP pulses were positioned on the GABA-H3 resonance at 1.89 ppm, while the intrapulse delay was adjusted to give full excitation at GABA-H4 at 3.01 ppm (intrapulse delay  $\sim 2.5 \text{ ms}$ ).

## RESULTS AND DISCUSSION

Figure 3 shows the performance of the editing sequences presented for the detection of GABA *in vitro*. For comparison the performance of “conventional”  $J$ -difference editing (5, 6) has also been measured and is shown in Fig. 3A. It can be seen that conventional  $J$ -difference editing recovers the complete outer resonances of GABA (and some of the inner resonance due to strong coupling effects) at the expense of incomplete water suppression. Furthermore, the amplitude of one of the two subspectra had to be corrected by 3% to obtain complete creatine suppression, due to limits on selectivity imposed by performing the editing pulse during the time allowed by the spin-echo period. The degree of amplitude correction is RF dependent, which complicates quantitation when a surface coil with an inhomogeneous RF distribution is used to apply the editing pulse. The iLSO sequence (Fig. 3B) provided excellent water suppression and spectral stability at the expense of a 50% signal reduction. Finally, the cLSO editing sequence (Fig. 3C) provided full signal recovery

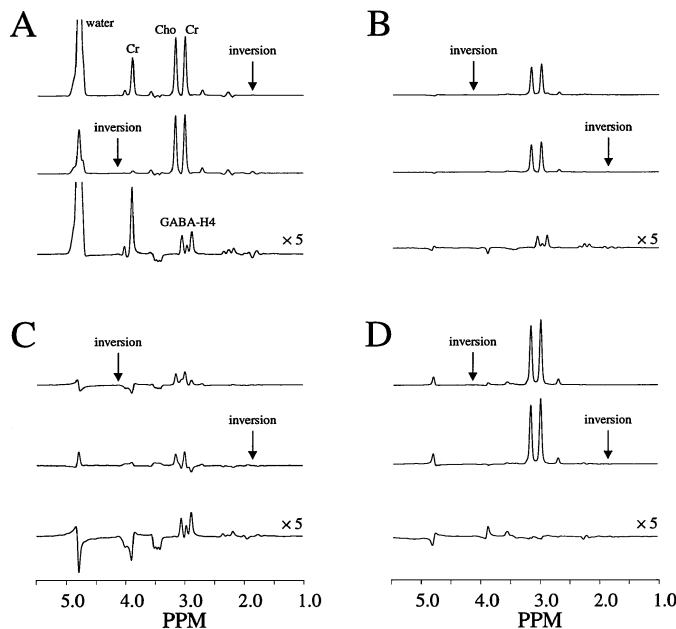


**FIG. 3.** *In vitro* spectral editing of  $\gamma$ -aminobutyric acid (GABA).  $^1\text{H}$  NMR spectra are acquired using (A) “conventional”  $J$ -difference editing, (B) iLSO editing, and (C,D) cLSO editing. The cLSO sequence was optimized for (C) GABA or (D) total creatine detection, respectively.

of the outer GABA resonances, excellent water suppression, and significant creatine (and choline) signal suppression in a single acquisition. Optimal creatine suppression was obtained when the relative phase between the first and second  $90^\circ$  pulses was  $10^\circ$ . The residual choline and creatine resonances are effectively eliminated in the edited difference spectrum. Almost complete creatine recovery is automatically obtained with a relative phase of  $100^\circ$  (Fig. 3D). The high-field approximation for GABA-H4 holds well for both sequences. Although the inner GABA-H4 resonance is partially edited, the outer resonances are generally partially suppressed, such that the experimental iLSO and cLSO editing efficiencies (as determined by integration) of  $24 \pm 2$  and  $46 \pm 3\%$  are close to the theoretical, high-field values of 25 and 50%, respectively. Full density matrix calculations (NMR-Sim, Bruker Analytik GmbH) of the iLSO and cLSO sequences for GABA reveal editing efficiencies of 24 and 44%, respectively.

The performance of the cLSO sequence is determined in part by the phase calibration of the second  $90^\circ$  pulse. When calibrated correctly, the sequence suppresses the overlapping tCr resonance completely in a single acquisition, while simultaneously recovering the outer resonances of GABA-H4. In the worse case, the phase is set  $90^\circ$  from the optimum and the GABA-H4 resonances are completely suppressed. In practice, the correct phase can be calibrated on the water resonance in a quick and reliable manner. Omitting the water suppression elements (but attaining the corresponding magnetic field gradients) and adjusting the frequency offset of the SSAP pulses to give maximum excitation of water, the phase angles can be accurately calibrated by maximizing or minimizing the water signal. In practice it was found that the

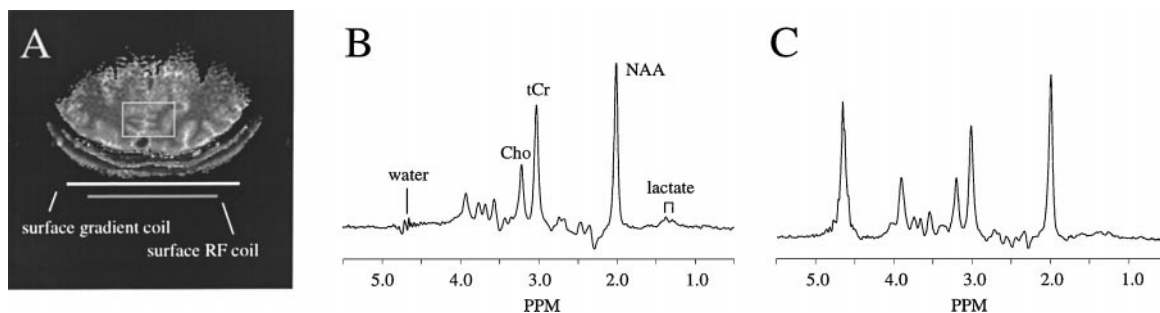


**FIG. 4.** *In vivo* evaluation of MEGA and WATERGATE water suppression. (A) Axial MR image displaying the position of the  $3 \times 2 \times 3$  cm<sup>3</sup> volume relative to the surface gradient and RF coils. <sup>1</sup>H NMR spectra obtained with (B) MEGA and (C) WATERGATE water suppression (TE = 68 ms).

expected sinusoidal signal dependence on the pulse phase was well attained and that the phase could be accurately determined in steps of 10°.

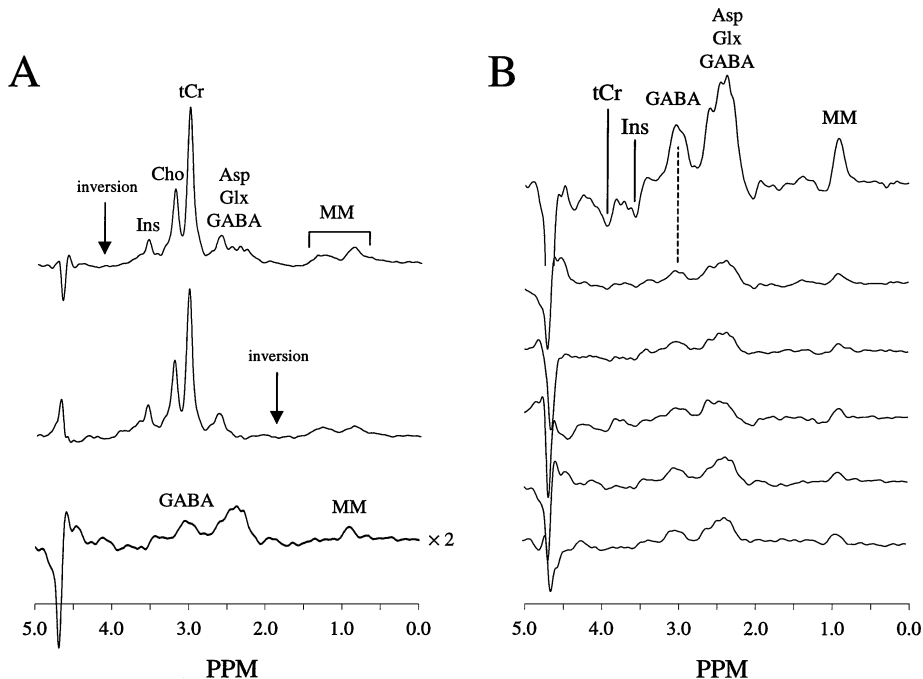
Employing adiabatic jump–return pulses significantly reduced the sensitivity toward RF inhomogeneities of both sequences. Unfortunately, it was not possible to execute the complete sequence with adiabatic RF pulses. Some RF pulses, like the slice-selective excitation pulse during iLSO editing, induce signal loss without introducing artifacts or affecting the editing performance. However, the performance of the selective inversion pulse used for editing purposes will affect the edited GABA signal intensity (relative to tCr). The effect of the selective inversion pulse on the edited GABA intensity was evaluated *in vitro* by varying the amplitude of the pulse. Varying the RF amplitude by  $\pm 3$  Db (in 1-Db steps) decreased the amplitude of the outer GABA resonances by  $>25\%$ . However, the inner GABA resonance more than doubled, such that the *integrated* GABA signal intensity remained constant within  $\sim 10\%$  over a  $\pm 3$  Db range. This effect is attributed to residual strong coupling on the GABA-H4 resonances and has been confirmed by density matrix simulations.

Figure 4 shows the *in vivo* performance of the two implemented water suppression techniques, MEGA (Fig. 4B) and WATERGATE (Fig. 4C). The <sup>1</sup>H NMR spectra are acquired from an 18-ml volume positioned in the occipital/parietal human cerebral cortex as indicated in Fig. 4A. Both techniques provided excellent and consistent water suppression. The adiabatic MEGA sequence generally provided more robust water suppression with minimal operator interaction, because MEGA (when executed with adiabatic RF pulses) does not require detailed RF power calibrations. The <sup>1</sup>H NMR spectra of Fig. 4 also indicate that the spatial localization, as achieved by OVS, ISIS, and 1D slice selection, was sufficient to discriminate the low-concentration lactate resonance from potentially overwhelming lipid resonances originating from extracranial regions.

Figure 5 shows the result for GABA detection in the occipital/parietal human cerebral cortex with the iLSO sequence. Similar to the results in Fig. 4, the water suppression in the individual subspectra is excellent. The NAA methyl protons are not observed due to the sinusoidal excitation profile of the

SSAP pulses that is centered at GABA-H3 (1.89 ppm). The edited spectrum shows a clear GABA resonance at 3.01 ppm, as well as coedited but nonoverlapping resonances from aspartate, GABA-H2, glutamate, glutamine, inositol, and macromolecules. Figure 5B shows the stability and reproducibility of the edited GABA spectra within a single volunteer as measured over a period of 48 h. The GABA and coedited resonances, as well as the water suppression, are extremely stable despite small changes in spatial position, shimming, and RF homogeneity. The top spectrum represents the sum of the five individual spectra and clearly displays the coedited resonances. The negative resonances of tCr and inositol are present due to the selective inversion pulse in the mirrored experiment (top spectrum, Fig. 5A). When the mirrored experiment is performed without a selective inversion pulse, no coedited resonances will be present between the chemical shifts of GABA-H4 and water.

Figure 6 displays the results for human brain GABA editing with the cLSO sequence. In order to establish the stability of the measurement and optimize the relative phase for GABA detection, the phase of the first SSAP pulse is set 90° from the optimum for GABA detection (Fig. 6A). As expected, the total creatine and choline resonances are almost completely retained, while the water is well suppressed. Performing the *J*-difference editing results in a clean subtraction of the total creatine and choline resonances to within the noise level. Setting the relative phase for optimal GABA detection (Fig. 5B) results in a near complete suppression of uncoupled resonances in the individual subspectra. The edited spectrum holds a clear GABA resonance at 3.01 ppm. The edited GABA signal-to-noise ratio is somewhat obscured by the presence of coedited, but nonoverlapping resonances. The actual signal-to-noise ratio of the integrated, edited GABA resonance, using the standard deviation over the real noise level (see inset), amounts to  $>40$ . It should be noted that complete suppression of uncoupled spins is only possible when (i) a perfect phase relation is attained between the first two 90° pulses and (ii) the nutation angle equals exactly 90°. Since a jump–return (or SSAP) pulse achieves excitation according to a sinusoidal frequency profile, the second criterion can never be satisfied for all resonances simultaneously. However, since GABA-H4 experiences a 90° nutation, the overlapping



**FIG. 5.** *In vivo* GABA detection by incoherent longitudinal scalar order (iLSO) difference editing. (A)  $^1\text{H}$  NMR subspectra obtained by the iLSO sequence (Fig. 2A) with the inversion pulse at 4.13 ppm (top) and at 1.89 ppm (GABA-H3, middle). The edited GABA spectrum (bottom) is calculated as the difference between the two subspectra. The edited GABA spectrum represents the sum of 512 accumulations acquired over  $\sim 25$  min. (B) GABA detection on a single subject over a period of 48 h. The bottom five spectra are acquired over  $\sim 25$  min each, while the top spectrum represents the sum of the five spectra.

total creatine resonance will be optimally suppressed. Other resonances, like choline, will be partially suppressed in a single acquisition and completely eliminated in the difference spectrum. Complete suppression of all resonances can theoretically

be achieved by replacing the jump–return (or SSAP) pulses by inherently refocused, frequency-selective RF pulses like E-BURP (13). However, since these pulses are nonadiabatic, they were not implemented for the studies described here.

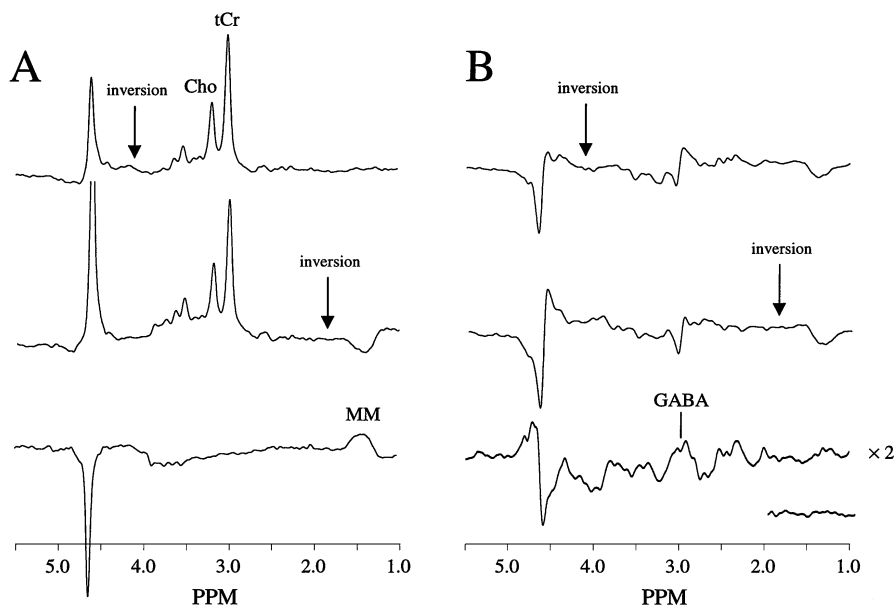


**FIG. 6.** *In vivo* GABA detection by coherent longitudinal scalar order (cLSO) difference editing. (A) cLSO editing optimized for detection of total creatine ( $\phi_1 = 0^\circ$ ,  $\phi_2 = 100^\circ$ ). The absence of GABA in the difference spectrum (bottom) ensures a correctly calibrated phase relation for optimal GABA detection with  $\phi_1 = 0^\circ$  and  $\phi_2 = 100^\circ - 90^\circ = 10^\circ$  (B). The inset displays the actual noise level of the cLSO-edited GABA spectrum.

The ratio of the integrated areas of edited GABA and total creatine as obtained with the iLSO sequence (Fig. 5) is equal to  $0.107 \pm 0.009$  over five measurements within one volunteer and  $0.115 \pm 0.018$  over three measurements in three different volunteers. The intra- and intersubject variations in (GABA/tCr) are therefore  $\sim 8$  and  $\sim 16\%$ , respectively. Using the (known) concentration of total creatine as an internal concentration reference, the GABA-tCr ratio can be converted to an absolute GABA concentration. No attempt toward absolute GABA quantification has been made here for the reason that the integrated GABA intensity and the GABA-tCr ratio are affected by several factors that must be measured separately. Specifically, the following points must be considered in attempting to measure absolute cerebral GABA concentrations. Firstly, the edited GABA resonance, although not contaminated by total creatine, is still a superposition of several metabolites, in particular GABA, homocarnosine, and in some cases glutathione. Homocarnosine is a dipeptide of GABA and histidine and is normally present at a concentration lower, but of comparable magnitude, than that of GABA. Because the chemical shifts and  $J$ -coupling constants of GABA-H4 and homocarnosine are identical, they cannot be discriminated by spectral editing. However, the imidazole protons in homocarnosine give distinct resonances at  $\sim 7$  and  $8$  ppm, which can be observed and quantified by short TE  $^1\text{H}$  MRS (24). Using appropriate conversion factors between the different detection methods (in terms of  $T_1$  and  $T_2$  relaxation), the homocarnosine contribution to the edited GABA intensity can be removed. At lower magnetic field strengths, additional contamination from glutathione may arise, although based on our measurements of the pure compound it will have a negligible contribution with the iLSO and cLSO sequences. The glutathione contribution reduces to zero when the second "mirror" experiment is performed without an inversion pulse.

Secondly, the GABA-H4 resonance coresonates with a macromolecular resonance M7 (25). Since M7 is coupled to a macromolecular resonance M4 at 1.71 ppm, it can potentially be coedited by the editing technique. The separation between M4 and GABA-H3 is only 0.18 ppm or  $\sim 16$  Hz at 2.1 T. With the spectral selectively used in previous studies at 2.1 T, the editing efficiency for macromolecules was approximately 65% of when the editing pulse is on resonance, resulting in the macromolecular resonance M7 accounting for  $\sim 40\%$  of the edited resonance intensity *in vivo* (6). Detailed *in vivo* experiments are required to establish the macromolecular contributions for the NMR sequences presented here. Based on simulations of editing selectivity, the theoretical editing efficiency for macromolecules with the iLSO sequence is  $\sim 55\%$ , implying an approximately 35% contribution to the edited resonance at 2.1 T. With increased chemical shift dispersion at 4 T the macromolecular contribution should decrease well below  $\sim 20\%$  (7, 8). Preliminary results obtained on rat brain at 7 T (data not shown) indicate that the increased spectral selectively effectively eliminates coediting of other reso-

nances to  $<5\%$  of the GABA-H4 resonance. At lower magnetic fields the remaining macromolecule intensity may be removed by nulling on the basis of differences in  $T_1$  relaxation times (25).

Thirdly, the general issues that affect quantitation in all *in vivo* NMR spectra must be taken into account. The GABA-H4 resonance intensity must be corrected for the effects of  $T_1$  and  $T_2$  relaxation, magnetization transfer, and diffusion. Furthermore, differences between the internal concentration standard tCr and GABA must be taken into account. Absolute GABA quantification is complicated by coediting of other resonances (at different chemical shifts), which as a result distort the baseline and make direct integration difficult. This problem can be solved by employing a spectral fitting algorithm like LCmodel (26), which uses prior knowledge on the chemical shifts,  $J$ -coupling constants, and patterns of the individual metabolites.

The described LSO sequences were implemented with ISIS/OVS localization because (i) ISIS and OVS are general localization techniques that can proceed any NMR sequence and (ii) the echo time was largely used for state-of-the-art water suppression techniques like MEGA (20) and WATERGATE (21). However, this localization strategy is only one of many possibilities and is not necessarily optimal under all conditions. For instance, when (macroscopic) motion is a significant factor, a single-scan localization sequence like PRESS is more suitable since this allows interscan phase and amplitude corrections. Both sequences are readily executed with PRESS, although time constraints force the iLSO sequence to be executed with WATERGATE water suppression.

Independent of the implemented localization technique, the LSO sequences can always be extended by 1D, 2D, or 3D phase-encoding gradients in order to obtain GABA spectroscopic images.

## CONCLUSION

We have described two novel editing sequences based upon longitudinal spin order, and demonstrated that it provides reliable *in vivo* detection of GABA with excellent water suppression and spatial localization at 2.1 T. Since spectral editing is achieved with longitudinal coherences, the sequences are extremely robust toward phase and/or frequency instabilities. Furthermore, the complete echo-time period can be used to achieve excellent water suppression with full insensitivity toward  $T_1$  relaxation using MEGA and WATERGATE. The cLSO sequence provides almost complete suppression of uncoupled resonances, like total creatine, in a single acquisition, thereby making the sequence robust toward motion. The spectral editing selectivity provided by applying the editing pulse during the period when the magnetization is in the LSO state results in relatively low coediting of nearby resonances of glutathione and macromolecules. At fields of 4 T and above, the sequence should be able to almost completely remove macromolecule overlap in the edited resonance.

## ACKNOWLEDGMENTS

The authors thank Drs. Kevin L. Behar and Ognen A. C. Petroff for helpful discussions. This research was supported by NIH Grant R29 NS32126-02.

## REFERENCES

1. A. McCormick, GABA as an inhibitory neurotransmitter in human cerebral cortex, *J. Neurophysiol.* **62**, 1018–1027 (1989).
2. B. S. Meldrum, GABAergic mechanisms in the pathogenesis and treatment of epilepsy, *Br. J. Clin. Pharmacol.* **27**, 3S-11S (1989).
3. G. Sanacora, G. F. Mason, D. L. Rothman, K. L. Behar, F. Hyder, O. A. C. Petroff, R. M. Berman, D. S. Charney, and J. H. Krystal, Reduced cortical gamma-aminobutyric acid levels in depressed patients determined by proton magnetic resonance spectroscopy, *Arch. Gen. Psych.* **56**, 1043–1047 (1999).
4. T. L. Perry, S. J. Kish, J. Buchanan, and S. Hansen,  $\gamma$ -Aminobutyric-acid deficiency in brain of schizophrenic patients, *Lancet* **1**, 237–239 (1979).
5. D. L. Rothman, K. L. Behar, H. P. Hetherington, and R. G. Shulman, Homonuclear  $^1\text{H}$  double resonance difference spectroscopy of the rat brain *in vivo*, *Proc. Natl. Acad. Sci. USA* **81**, 6330–6334 (1984).
6. D. L. Rothman, O. A. C. Petroff, K. L. Behar, and R. H. Mattson, Localized  $^1\text{H}$  NMR measurements of  $\gamma$ -aminobutyric acid in human brain *in vivo*, *Proc. Natl. Acad. Sci. USA* **90**, 5662–5666 (1993).
7. H. P. Hetherington, B. R. Newcomer, and J. W. Pan, Measurements of human cerebral GABA at 4.1 T using numerically optimised editing pulses, *Magn. Reson. Med.* **39**, 6–10 (1998).
8. M. Mescher, H. Merkle, J. Kirsch, M. Garwood, and R. Gruetter, Simultaneous *in vivo* spectral editing and water suppression, *NMR Biomed.* **11**, 266–272 (1998).
9. J. R. Keltner, L. L. Wald, B. Frederick, and P. Rensaw, *In vivo* GABA detection in human brain using a localized double-quantum filter technique, *Magn. Reson. Med.* **37**, 366–371 (1997).
10. J. Shen, D. C. Shungu, and D. L. Rothman, *In vivo* chemical shift imaging of  $\gamma$ -aminobutyric acid in the human brain, *Magn. Reson. Med.* **41**, 35–42 (1999).
11. R. Reddy, V. H. Subramanian, B. J. Clark, and J. S. Leigh, Longitudinal spin-order based pulse sequence for lactate editing, *Magn. Reson. Med.* **19**, 477–482 (1991).
12. R. Reddy, V. H. Subramanian, B. J. Clark, and J. S. Leigh, *In vivo* lactate editing in the presence of inhomogeneous  $B_1$  fields, *J. Magn. Reson. B* **102**, 20–25 (1993).
13. R. A. de Graaf, “*In vivo* NMR Spectroscopy. Principles and techniques.” Wiley, Chichester (1998).
14. O. Sørensen, G. Eich, M. Levitt, G. Bodenhausen, and R. R. Ernst, Product operator formalism for the description of NMR pulse experiments, *Prog. NMR Spectrosc.* **16**, 163–192 (1983).
15. R. Gruetter, Automatic, localized *in vivo* adjustment of all first- and second-order shim coils, *Magn. Reson. Med.* **29**, 804–811 (1993).
16. J. Shen, R. E. Rycyna, and D. L. Rothman, Improvements on an *in vivo* automatic shimming method [FASTERMAP], *Magn. Reson. Med.* **38**, 834–839 (1997).
17. R. J. Ordidge, A. Connelly, and J. A. B. Lohman, Image-selected *in vivo* spectroscopy (ISIS). A new technique for spatially selective NMR spectroscopy, *J. Magn. Reson.* **66**, 283–294 (1986).
18. W. Chen, and J. J. Ackerman, Spatially-localized NMR spectroscopy employing an inhomogeneous surface-spoiling magnetic field gradient. 1. Phase coherence spoiling theory and gradient coil design, *NMR Biomed.* **3**, 147–57 (1990).
19. A. Haase, J. Frahm, W. Hanicke, and D. Matthaei,  $^1\text{H}$  NMR chemical shift selective (CHESS) imaging, *Phys. Med. Biol.* **30**, 341–344 (1985).
20. M. Mescher, A. Tannus, M. O’Neil Johnson, and M. Garwood, Solvent suppression using selective echo dephasing, *J. Magn. Reson. A* **123**, 226–229 (1996).
21. V. Sklenar, M. Piotto, R. Leppik, and V. Saudek, Gradient-tailored water suppression for  $^1\text{H}$ - $^{15}\text{N}$  HSQC experiments optimized to retain full sensitivity, *J. Magn. Reson. A* **102**, 241–245 (1993).
22. T. L. Hwang, P. C. M. van Zijl, and M. Garwood, Asymmetric adiabatic pulses for NH selection, *J. Magn. Reson.* **138**, 173–177 (1999).
23. R. A. de Graaf, Y. Luo, M. Terpstra, H. Merkle, and M. Garwood, A new localization method using an adiabatic pulse, BIR-4, *J. Magn. Reson. B* **106**, 245–252 (1995).
24. D. L. Rothman, K. L. Behar, J. W. Prichard, and O. A. C. Petroff, Homocarnosine and the measurement of neuronal pH in patients with epilepsy, *Magn. Reson. Med.* **32**, 924–929 (1997).
25. K. L. Behar, D. L. Rothman, D. D. Spencer, and O. A. C. Petroff, Analysis of macromolecule resonances in  $^1\text{H}$  NMR spectra of human brain, *Magn. Reson. Med.* **32**, 294–302 (1994).
26. S. W. Provencher, Estimation of metabolite concentrations from localized *in vivo* proton NMR spectra, *Magn. Reson. Med.* **30**, 672–679 (1993).